



Contents lists available at ScienceDirect

Saudi Journal of Biological Sciences

journal homepage: www.sciencedirect.com

Original article

Comparative analysis of PHAs production by *Bacillus megaterium* OUAT 016 under submerged and solid-state fermentationS. Mohapatra^a, S. Pattnaik^b, S. Maity^c, S. Mohapatra^d, S. Sharma^e, J. Akhtar^f, S. Pati^b, D.P. Samantaray^{b,*}, Ajit Varma^a^a Department of Microbial Technology, Amity University Utter Pradesh, Noida, India^b Department of Microbiology, OUAT, Bhubaneswar, Odisha, India^c University Innovation Cluster Biotechnology, University of Rajasthan, Rajasthan, India^d Department of Economics, OUAT, Bhubaneswar, Odisha, India^e Department of Mechanical Engineering, Amity University, Noida, India^f IMGEX India Private Limited, Bhubaneswar, Odisha, India

ARTICLE INFO

Article history:

Received 27 September 2019

Revised 28 January 2020

Accepted 1 February 2020

Available online 17 February 2020

Keywords:

PHAs

Bacillus megaterium

PHB-co-PHV

DTA

AFM

ABSTRACT

In view of risk coupled with synthetic polymer waste, there is an imperative need to explore biodegradable polymer. On account of that, six PHAs producing bacteria were isolated from mangrove forest and affiliated to the genera *Bacillus* & *Pseudomonas* from morpho-physiological characterizations. Among which the potent PHAs producer was identified as *Bacillus megaterium* OUAT 016 by 16S rDNA sequencing and *in-silico* analysis. This research addressed a comparative account on PHAs production by submerged and solid-state fermentation pertaining to different downstream processing. Here, we established higher PHAs production by solid-state fermentation through sonication and mono-solvent extraction. Using modified MSM media under optimized conditions, 49.5% & 57.7% of PHAs were produced in submerged and 34.1% & 62.0% in solid-state fermentation process. Extracted PHAs was identified as a valuable polymer PHB-co-PHV and its crystallinity & thermostability nature was validated by FTIR, ¹H NMR and XRD. The melting (*T_m*) and thermal degradation temperature (*T_d*) of PHB-co-PHV was 166 °C and 273 °C as depicted from DTA. Moreover, FE-SEM and SPM surface imaging indicated biodegradable nature, while FACS assay confirmed cytocompatibility of PHB-co-PHV.

© 2020 The Authors. Published by Elsevier B.V. on behalf of King Saud University. This is an open access article under the CC BY-NC-ND license (<http://creativecommons.org/licenses/by-nc-nd/4.0/>).

1. Introduction

Petrochemical based polymer is a matter of great concern due to its detrimental consequence on the environment, which demands a need to develop alternate biodegradable polymer. The eco-friendly polymer is nothing but polyhydroxyalkanoates (PHAs) synthesized by a wide array of Gram-positive and negative bacteria (Mohapatra et al., 2015b) and accumulated as carbon & energy storage inclusion in the cytoplasm. The PHAs granule is synthesized under certain stress conditions such as nitrogen, phosphorus,

trace elements and oxygen (Mohapatra et al., 2016a). In particular, more than 150 different monomers of PHAs have been reported (Tan et al., 2014) from bacteria that are water-insoluble, UV resistant, non-toxic, impermeable to oxygen, biodegradable and biocompatible (Mayeli et al., 2015). These polymers have multifarious applications such as domestic plastic, skin tissue & other implants, drug coating, 3D printing in various photographic materials, nutritional dietary supplements, drugs and minute chemical substances (Maity et al., 2017).

Till date, the commercial PHAs production is exclusively dependent upon Gram-negative bacteria. However, production of endotoxin based PHAs by these bacteria holds back its successful commercialization and diverse biomedical applications (Sultanpuram et al., 2010). As a matter of fact, the genus *Bacillus* is widely used by academia due to their faster generation time, genomic stability, utilization of economical substrate that provides carbon resources for the production of endotoxin-free PHAs for different biomedical applications. Thus, for successful commercialization of endotoxin-free PHAs production, more efforts are

* Corresponding author.

E-mail address: dpsamantaray@yahoo.com (D.P. Samantaray).

Peer review under responsibility of King Saud University.



Production and hosting by Elsevier

indispensable to make the bioprocess technology, such as, submerged and solid-state fermentation process economically viable in contrast to both upstream and downstream processing. In addition, 50% costs of PHAs production crucially depends on upstream processing and the rest on downstream processing (Gomaa, 2014; Kunasundari and Sudesh, 2011). Nevertheless, inadequate research reports are available in the public domain for recovery of endotoxin-free PHAs produced under submerged and solid-state fermentation process by *Bacillus* species. In this research, we analyzed the quality and quantity of endotoxin free PHAs produced by *Bacillus megaterium* under submerged and solid-state fermentation process with special reference to downstream processing.

2. Materials and methods

2.1. Cultivation and screening of PHAs producers

Sediment samples were collected aseptically from the Bhitarkanika mangrove forest (19N & 22N and between 85E & 87E) of Odisha, India and processed in the laboratory for cultivation of aerobic heterotrophic bacteria using standard bacteriological techniques. Cultivated bacterial isolates were then induced for synthesis & accumulation of PHAs granules using minimal salt medium (2% glucose) and incubated at 37 °C for 24–72 h for screening of PHAs producer.

Subsequently, intracellular PHAs granule accumulation by bacteria were detected by Sudan black B followed by Nile blue staining under bright-field microscopic (1000X, Leica DM5000B) and UV-trans illuminator imaging (Maity et al., 2017). Further, PHAs accumulation and morphological (cell shape and size) transformation of bacteria during growth at different time interval was observed through field emission scanning electron microscopic (FE-SEM) imaging (Quanta 200 FEG) (Bhagowati et al., 2015). For conformation, transmission electron microscopic (TEM) (JEOL JEM 1200, JEOL Ltd., Tokyo, Japan) imaging was also conducted for detection of intracellular PHAs granule in the bacterial cytosol (Mohapatra et al., 2016a).

2.2. Morpho-physiological characterization

The morpho-physiological characterization of selected PHAs producers were studied based on standard bacteriological tests prescribed in Bergey's manual of determinative bacteriology. The selected bacterial isolates were subjected to morphological, biochemical, enzymatic, sugar utilization and antibiotic sensitivity tests for generic level identification (Holt et al., 1994).

2.3. Evolutionary analysis of the bacterial isolate

PCR amplified 16S rDNA product was sent to Eurofin Genomics Pvt. Ltd., Bangalore, India and sequenced with 16SF (5' AGAGTTT-GATCCTGGCTCAG 3') and 16SR (3' AAGGAGTGATCCACCGCA 5') primer using ABI 3730xl genetic analyzer (Mohapatra et al., 2016a). Consensus sequence was analyzed by bio-edit software (v7.0.5.3) and submitted to NCBI (<http://blast.ncbi.nlm.nih.gov/blast.cgi>) to get accession number. Alignment of desired *Bacillus* sp. and its closely related homologous 16S rDNA sequences were carried out by using ClustalW (v1.6) for evolutionary analysis. The phylogenetic tree was constructed by neighbour-joining method (Saitou and Nei, 1987) using MEGA v7.0 (Molecular Evolutionary Genetics Analysis) software (Tamura et al., 2013). The tree topologies were evaluated by bootstrap analysis (1000 replications). Further, secondary structure analysis of rRNA was conducted by M-fold web server (<http://www.bioinfo.rpi.edu/>

[application/mfold](#)) (Mathews and Turner, 2002) to get more stable structure of RNA with lowest free energy (Mohapatra et al., 2016a).

2.4. Optimization of growth parameters for higher biomass and PHAs yield

Bacterial cell biomass yield is regulated by several growth parameters. Further, PHAs production is parallel to bacterial cell biomass yield. Thus, growth parameters like cultivation medium, pH, temperature, carbon & nitrogen source & their concentration and inoculum size for PHAs producing bacteria were optimized by one factor at a time (OFAT) approach (Maity et al., 2017). As the primary growth factor, culture medium such as growth and modified minimal salt medium were prepared, 1.7×10^8 cells/ml of starter culture (0.5 McFarland standards) was inoculated and incubated at 37 °C for 24 h. Then, optimum bacterial cell biomass yield was estimated by measuring OD at 600 nm using UV-Vis spectrophotometer (λ 35-Perkin-Elmer). Culture medium depicting higher bacterial cell biomass yield was kept constant and then other parameters including pH (5–9), temperature (25–55 °C), carbon source (maltose, lactose, sucrose, glucose, fructose), glucose concentration (1–5%), nitrogen sources (NH_4Cl , KNO_3 , urea, $(\text{NH}_4)_2\text{SO}_4$), $(\text{NH}_4)_2\text{SO}_4$ (1–3 g/l) and inoculum age (5–30 h) were varied one by one sequentially. Then, the data obtained from the optimization studies were again validated by statistical analysis ($p < 0.5$).

2.5. PHAs production and extraction

PHAs production was carried out by submerged and solid-state fermentation process under optimized condition. Submerged fermentation was accomplished through one stage batch cultivation method (Singh et al., 2013). In brief, 1L of modified minimal salt medium (KH_2PO_4 0.5 g/l, K_2HPO_4 0.5 g/l, glutamic acid 1.5 g/l, malic acid 2.7 g/l, yeast-extract 4 g/l, glucose 30 g/l, NaCl 10 g/l, $(\text{NH}_4)_2\text{SO}_4$ 2.5 g/l) at pH 8.0 was inoculated with 20 h of inoculum age (1.5×10^8 cells/ml) and incubated at 35 °C/ 72 h. Correspondingly, solid-state fermentation process was conducted by lawn culture method (Sharma and Bajaj, 2016). In the solid-state fermentation process, nutritionally inert material agar was used as a carrier that imparts solid support for attachment of bacteria. Briefly, 1L of modified minimal salt agar medium with pH 8.0 was taken in 50 different plates, 20 h of inoculum age (0.1 ml/ plate & 1.5×10^8 cells/ml) was spread on the plate and incubated at 35 °C/ 72 h. Cell biomass was then collected and PHAs was recovered by following different downstream processing like sonication-mono-solvent and sodium hypochlorite digestion-multi-solvent extraction as described earlier (Singh et al. 2009; Arikawa et al., 2017).

2.6. Structural and thermal characterization of PHAs

2.6.1. FTIR

FTIR spectroscopic analysis was conducted to determine the functional group of PHAs. Extracted PHAs film (2 mg) was placed on a diamond-based plate of ATR (attenuated total reflectance). Then, IR spectra were recorded using single beam spectrometer (Perkin- Elmer RX I) within the scanning range $4000\text{--}400\text{ cm}^{-1}$ (Mohapatra et al., 2014).

2.6.2. NMR

^1H NMR was carried out to elucidate the proton configuration and its sequence distribution in the polymer chain of PHAs. Briefly, extracted PHAs film (10 mg/ml) was dissolved with CdCl_2 (1 ml) and subjected to NMR (JEOL JNM-LA). NMR spectra were recorded at 500 MHz with 5 ms pulse width, 32,000 data points and 32 accumulations were collected (Wang et al., 2016).

2.6.3. XRD

Structural integrity (degrees of crystallinity) of extracted PHAs was analyzed by X-ray diffractometer (PANalytical). PHAs sample was used in a capillary (d; 2 mm) tube, data were recorded in 2 θ range (2–30°), scan rate (2° /min) with nickel filtered Cu-K- α (λ = 0.1542 nm) beam and operated at 30 kV (Wang et al., 2016).

2.7. Thermal characterization of PHAs

Thermostability of PHAs was determined by differential thermo analysis (DTA) for its processing & application. Extracted PHAs was subjected to DSC Q20 and TGA Q50 analyzer for thermal analysis. Moisture free purified PHAs (10 mg) was taken with a sequential program of heating (heating rate 10 °C/min and temperature range 0 to 600 °C) in the presence of N₂ flow of 200 ml/min. Then, melting temperature (*T_m*), degradation temperature (*T_d*), glass transition temperature (*T_g*) and enthalpy of fusion (ΔH_m) of PHAs was recorded. Crystallinity (*X_c*) of PHAs was calculated by;

$$X_c \% = \frac{\Delta H_f}{\Delta H_f^\circ} \times 100$$

(ΔH_f = heat of fusion of PHAs and ΔH_f° = 146 J/g, the heat of fusion of standard PHB, the most common homopolymer of PHAs) (Wang et al., 2016).

2.8. Morphological analysis of PHAs film

Surface morphological properties of PHAs film was observed under field emission scanning electron microscopic (FE-SEM) and atomic force microscopic (AFM) (Shrivastav et al., 2014) imaging. In brief, extracted PHAs films were fixed on aluminum stumps, followed by gold coating through Polaron SC7620 sputter coater for FE-SEM (QUANTA 200 FEG, Netherlands). Correspondingly, aluminum stumps fixed PHAs film was processed for AFM imaging and surface morphology was studied using surface probe & laser beam.

2.9. Cytotoxicity assay of PHAs

Cytocompatibility of extracted PHAs was evaluated by cytotoxicity assay along with standard PHB (Sigma Aldrich, USA). In brief, 10% (w/v) each of extracted PHAs and standard PHB solutions with concentration from 100 to 500 μ g/ml were prepared with chloroform. Extracted polymer (PHB-co-PHV) film was cast in 24 well tissue culture plates and then seeded with adherent mouse fibroblast 3 T3 cell line (10⁶ cells/well). Cell culture was maintained in the Dulbecco's Modified Eagle Medium (DMEM) for 24 h [10% FBS, 2 mM glutamine and 1X antibiotic-antimycotic solution (Invitrogen, USA)]. Cells were collected with Trypsin-EDTA and survivability was estimated by propidium iodide (0.2 μ g/10⁶ cells) staining. Data acquisition was conducted by fluorescent activated cell sorting FACS caliber (BD) using cell quest software.

3. Result and discussion

3.1. Screening and morpho-physiological characterization of PHAs producing bacteria

Although earlier studies reported that a wide array of bacterial species produces biopolymer (PHAs), the sheer diversity of the microbial world attracts for exploration of high PHAs yielding bacteria from different ecological niches. In light of the above, 06 PHAs producing bacteria were isolated from the rich, lush green, vibrant ecosystem, Bhitarkanika mangrove forest of Odisha, India. These bacterial isolates were capable of accumulating PHAs granule as

carbonosome which was primarily confirmed by Sudan black staining (Fig. 1a). Among all, the bacterial isolate (SP8) was selected for PHAs production based on high intensity of light emitted under Nile red staining (Fig. S1, Supplementary file). The bacterial isolate was affiliated to genus *Bacillus* sp. (SP8) based on morpho-physiological, biochemical, sugar utilization and antibiotics characterization (Fig. S2, Table S1 & Table S2, Supplementary file). Rod shape and smooth cell surface of the screened bacteria was confirmed by FE-SEM. Notably, rod shape of the bacteria transformed to marginally oval due to increase in number and size of PHAs granules accumulated (Fig. 2) in the cytosol.

Similar shape changes in *Lysinibacillus* sp. 3HHX (Mohapatra et al., 2016b), *Bacillus* sp. CS-605 & *Bacillus cereus* AC-1 (Bhagowati et al., 2015) and *Cupriavidus necator* (Mravec et al., 2016) were observed during accumulation of PHAs granule. Moreover, the earlier report also suggested that long rod shapes of *Bacillus megaterium* facilitated the accumulation of a maximum number of PHAs granule as compared to other *Bacillus* species (Wu et al., 2016). In contrast to our observation, similar PHAs producing *Bacillus* species were also found in numerous environmental niches such as waste-water, sludge and marine ecosystems (Mohapatra et al., 2015b); (Bhagowati et al., 2015); (Pandian et al., 2010). This fact can be correlated with high organic carbon and less nitrogen, phosphorus, potassium content of the Bhitarkanika mangrove forest sediment is due to either direct incorporation of organic matter generated from anthropogenic activity or decomposition of plant materials (Thatoi et al., 2012), which creates a selective pressure for formation of PHAs granules (Mohapatra et al., 2015b). Moreover, *Bacillus* is the predominant genera of soil, genetically stable, generally regarded as safe and capable of growing in presence of cheap raw materials than other bacterial isolates (Khyami et al., 2011). Here, we explored for the first time PHAs producing *Bacillus* sp. from the Bhitarkanika mangrove forest.

3.2. Evolutionary analysis of the bacterial isolate

The predicted neighbour joining (NJ) based phylogenetic tree (Fig. 3) with the sum of branch length 0.02 depicted an evolutionary relationship among isolated bacterial strain *Bacillus* sp. OUAT 016 with other eight closely related 16S rDNA sequences belonging *Bacillus* species retrieved from NCBI database. The sequences are clustered into one major group and diverged distinctly from the outgroup (*Pseudomonas aeruginosa* KAVK01). There are two sub-groups are present within the major group, where all nine bacterial strains are clustered together. In sub-group I bacterial strain such as *Bacillus* sp. OUAT 016 (MF276772), *Bacillus megaterium* BAB 2865 (KF853109), *Bacillus megaterium* B2P2 (EU221370) and *Bacillus megaterium* IHB 4625 (KF475802) whereas, in sub-group II *Bacillus megaterium* IHB 7295 (KJ767362), *Bacillus megaterium* H 1 (KT273285), *Bacillus megaterium* Jz11 (JF833087), *Bacillus megaterium* BMN1 (KJ461522), *Bacillus megaterium* S20718 (KF956607) are clustered together. Moreover, our desired bacterial strain *Bacillus* sp. OUAT 016 (MF276772) and *Bacillus megaterium* BAB 2865 (KF853109) strains are strongly related to each other within the sub-group I. On the other hand, *Bacillus megaterium* B2P2 (EU221370) and *Bacillus megaterium* IHB 4625 (KF475802) strains are related to each other under sub-group I. However, within the sub-group II, all the bacterial strains seem to be related to each other without any divergence. The PHAs producing bacterial strain was identified as *Bacillus megaterium* OUAT 016 by *in silico* analysis with Gen-bank accession numbers MF276772. Strong evolutionary relationship of *Bacillus megaterium* OUAT 016 with other closely related strains of *Bacillus megaterium* was also confirmed from secondary rRNA structure in terms of the highly conserved loop and stem. The bacterium is energetically (free energy –583 kcal/mol)

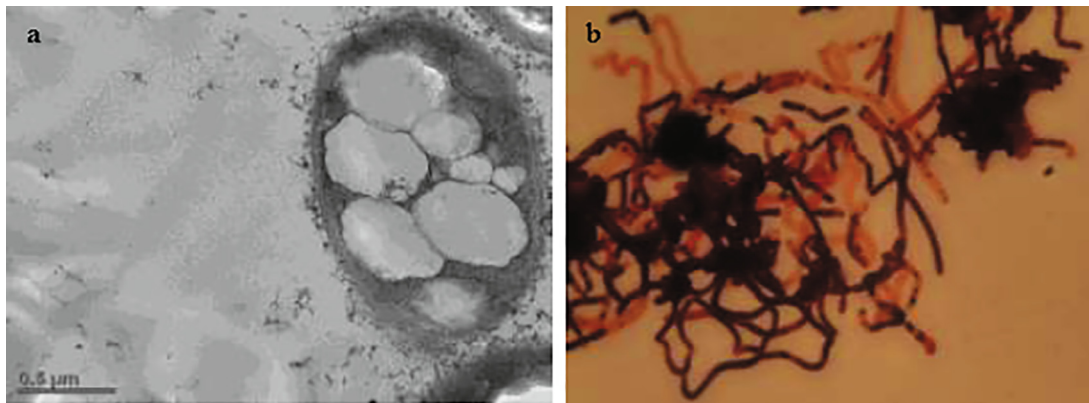


Fig. 1. PHAs accumulated *B. megaterium* OUAT 016 cells (a) under TEM and (b) BFM.



Fig. 2. Morphological modification (a, b & c) of *B. megaterium* OUAT 016 cell during PHAs accumulation from 24 to 72 h.

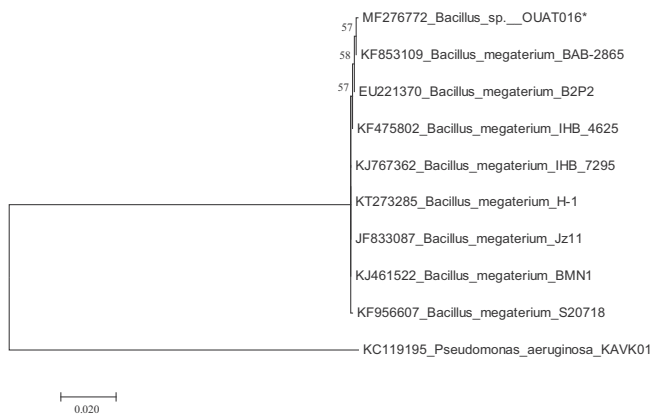


Fig. 3. Phylogram of *B. megaterium* OUAT 016 with its homologous sequences of BLAST search analysis.

stable (Fig. S3 & Table S3, Supplementary file) as confirmed from secondary rRNA structure analysis.

3.3. PHAs production

Growth parameters play a key role in biomass as well as PHAs production by bacteria *in-vitro*. Optimization study revealed higher cell biomass production in modified minimal salt medium at pH 8.0, temperature 35 °C, glucose 3% as carbon source, (NH₄)₂SO₄ (2.5 g/l) as nitrogen source and 20 h inoculum age were optimum at P < 0.05 significance level (Fig. S4a–g, Supplementary file). Under submerged fermentation, *Bacillus megaterium* OUAT016 produced 1.98 g/l and 2.31 g/l of PHAs from 4.0 g of dry cell weight (DCW) in 72 h by sodium hypochlorite digestion multi-solvent and sonication mono-solvent extraction method. Correspondingly,

in solid-state fermentation 2.05 g/l and 3.72 g/l of PHAs were produced from 6.0 g of DCW in 72 h. Comparatively, higher PHAs production (62%) was obtained in solid-state fermentation than submerged fermentation (57.7%). Interestingly, sonication mono-solvent was proved to be an efficient method for PHAs recovery in both cases.

Several reports are available in support of PHAs production such as 2.5 g/l by *Bacillus* sp. S1 2013b (Mohapatra et al., 2014), 1.62 g/l by *Bacillus subtilis* KP172548 (Mohapatra et al., 2017b), 4.1 g/l by *Bacillus thuringiensis* KJ206079 (Desouky et al., 2014), 1.60 g/l by *Bacillus megaterium* (Israni and Shivakumar, 2013), 3.0 g/l by *Bacillus cereus* SPV (Valappil et al., 2007) and 6.07 g/l by *Bacillus* sp. (Musa et al., 2016) under submerged fermentation through sodium hypochlorite digestion multi-solvent extraction. So far our knowledge is concerned, inadequate attention has been provided towards the recovery of PHAs using mono-solvent extraction method. An earlier report (Arikawa et al., 2017) suggested that *C. necator* KNK-005 produced 15.6 g/l of PHAs from 18.6 g/l of biomass DCW under submerged fermentation through sonication mono-solvent extraction method. Besides submerged fermentation, solid-state fermentation can be used as an alternative strategy for PHAs production (Sindhu, 2015). As a matter of fact, *Bacillus sphaericus* NII0838 (Ramadas et al., 2009) and *Bacillus megaterium* MSBN04 (Sathiyarayanan et al., 2013) produced 0.169 g/l and 8.637 g/l of PHAs under solid-state fermentation through sodium hypochlorite digestion multi-solvent extraction. Notably, research findings are not available on the recovery of PHAs by sonication mono-solvent extraction under solid-state fermentation using *Bacillus* species. Here, we report for the first time higher PHAs recovery through sonication mono-solvent extraction, which prevent degradation of PHAs and reduction in molecular weight as compared to sodium hypochlorite digestion multi-solvent extraction method (Rawte and Mavinkurve, 2002).

3.4. Structural and thermal analysis of PHAs

3.4.1. FTIR analysis

FTIR spectra showed four intense absorption bands at 1181, 1379, 1452 and 1261 cm^{-1} corresponding to $\text{R-CO-O-C}_2\text{H}_5$

stretch, $-\text{CH}_3$, $-\text{CH}_2$, and $-\text{CH}$ groups respectively (Fig. 4). However, the high intense absorption band obtained at 1719.36 cm^{-1} assigned to the C=O stretch mode of crystalline parts in PHB-co-PHV (Fig. 4). These major annotated vibrational peaks were also comparable with the peaks of PHB-co-PHV as reported earlier

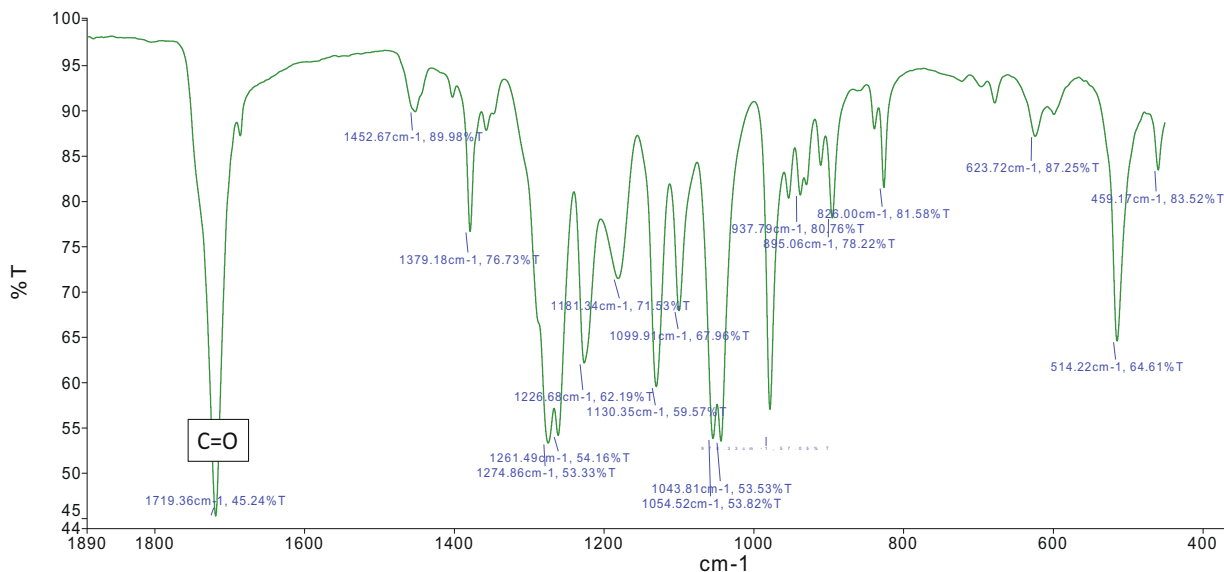


Fig. 4. FTIR spectra at 1719.36 cm^{-1} depicting C=O functional group of PHAs.

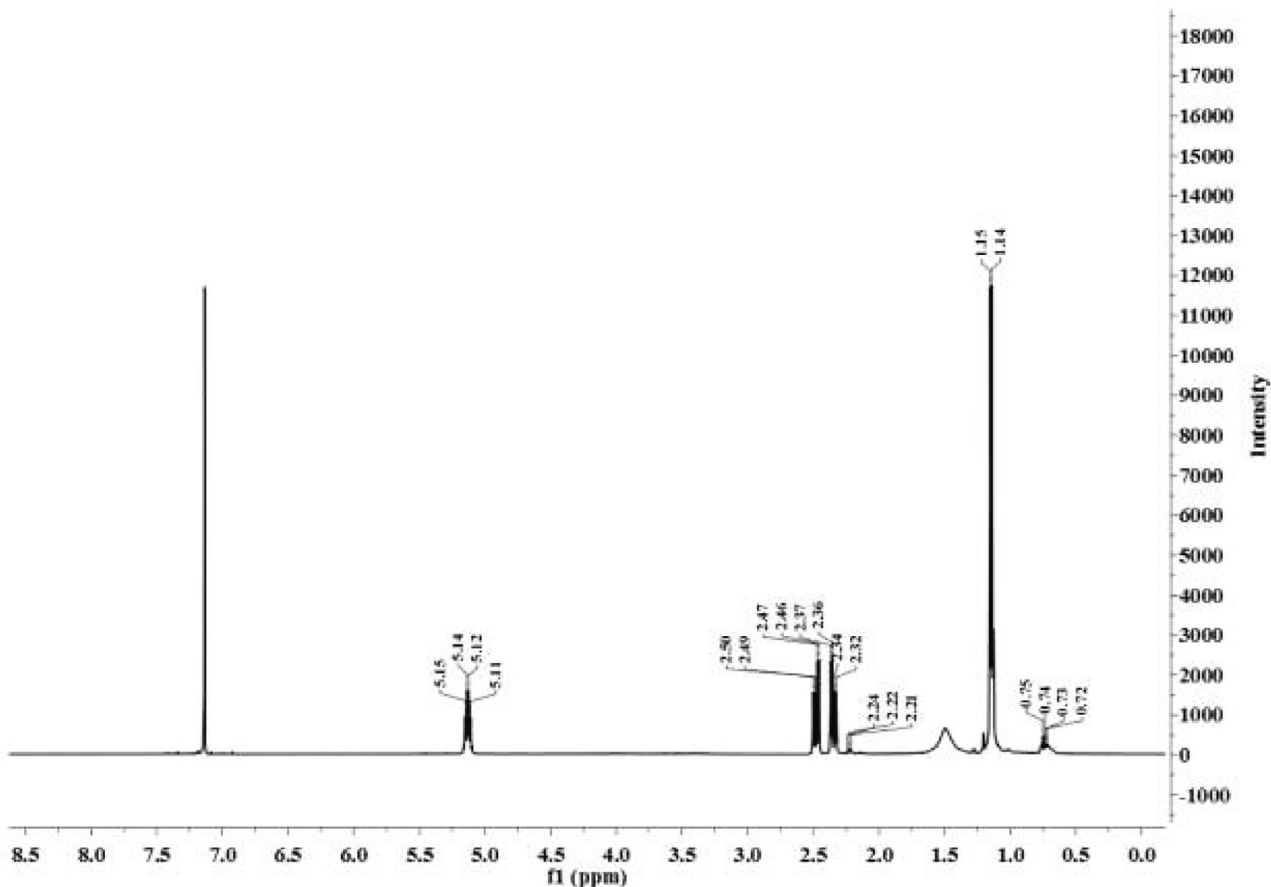


Fig. 5. ^1H NMR chemical shift pattern established the extracted polymer is a co-polymer PHB-co-PHV.

(Wang et al., 2016; Masood et al., 2012). Thus, IR analysis provided a correct insight for the chemical structure of PHB-co-PHV by reflecting the monomeric units that are predominantly present in the PHAs.

3.4.2. ^1H NMR analysis

^1H NMR spectroscopic (Fig. 5) patterns of various chemical shifting values ranging from 0.72 to 0.75 ppm correspond to the methyl terminal groups of 3HV monomer unit. Apart from that

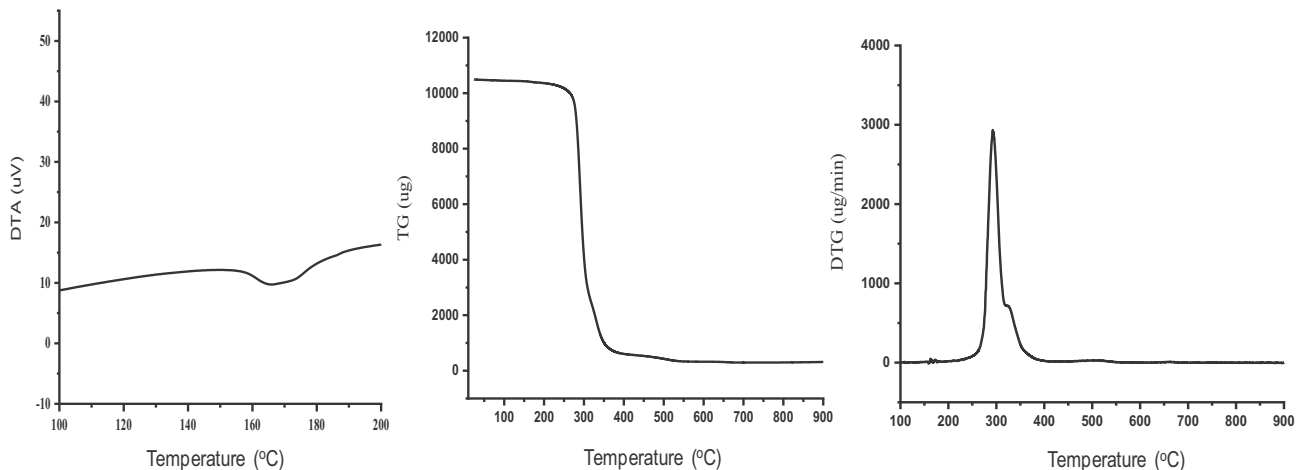


Fig. 6. DTA elucidating melting (T_m -166 °C) and thermal degradation (T_d -273 °C) temperature of PHB-co-PHV.

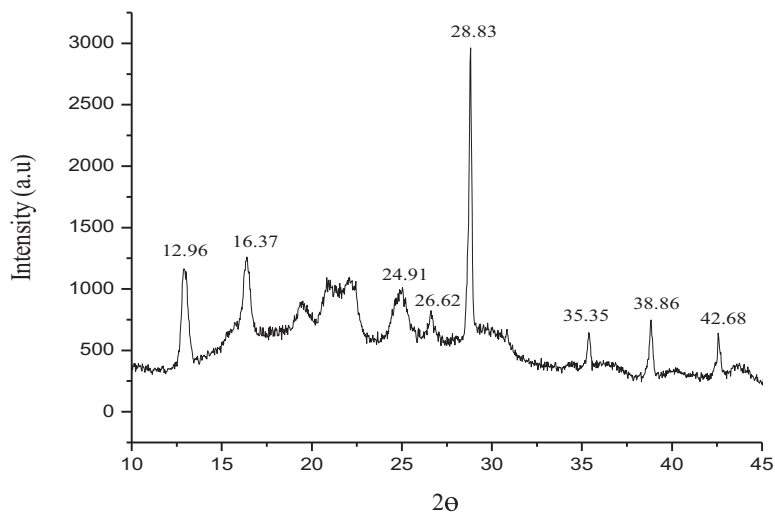


Fig. 7. X-ray diffractogram indicating crystalline nature of PHB-co-PHV.

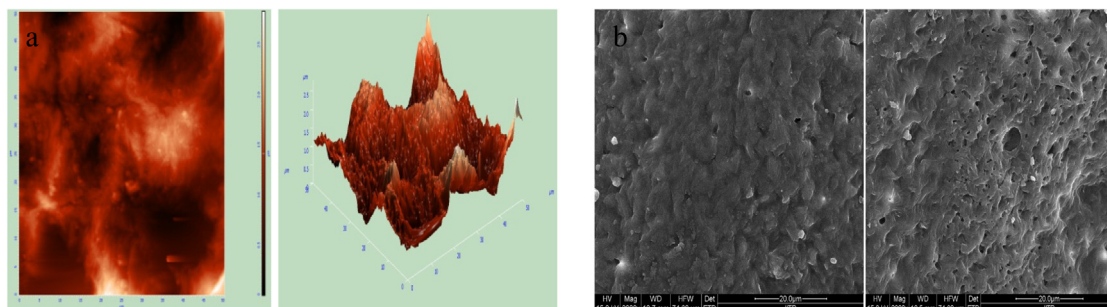


Fig. 8. Surface morphology of PHB-co-PHV film under (a) AFM and (b) FE-SEM.

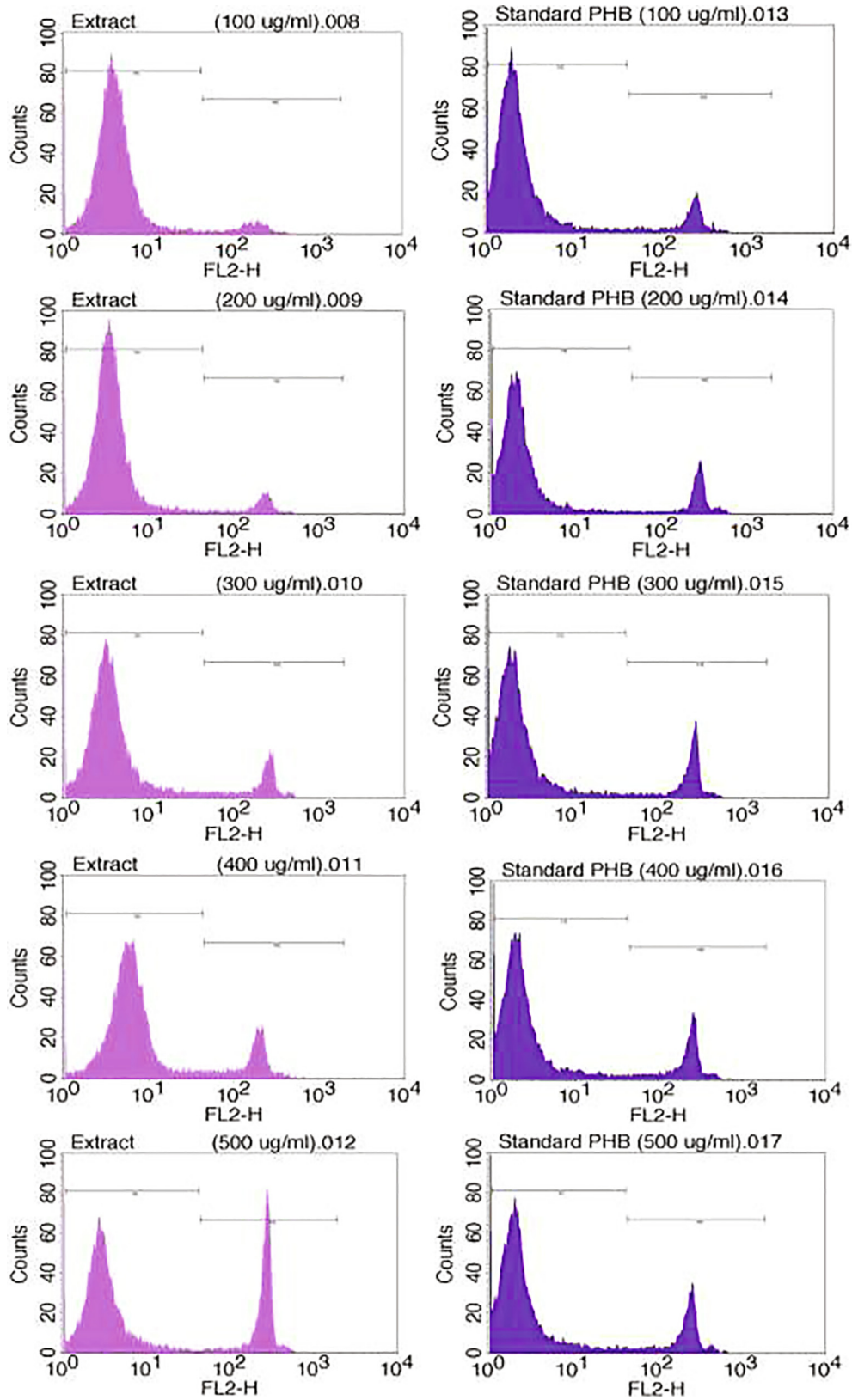


Fig. 9. Comparative cytotoxicity assay of extracted PHB-co-PHV and standard PHB.

doublet at 1.14, 1.15 ppm corresponds to $-\text{CH}_3$, small multiplet peaks at 2.21–2.24 ppm and quadrate of doublet peaks at 2.32–2.50 ppm indicates $-\text{CH}_2$ group of HV & HB present in the PHAs polymer. Another chemical shift at 5.11–5.15 ppm denotes pres-

ence of $-\text{CH}$ group in the extracted polymer. The ^1H NMR spectrum of the purified polymer was consistent with previous findings of other studies. More specifically, the presence of valerate monomer in the polymer was confirmed by the existence of $-\text{CH}_3$

at 0.9 & 0.92 ppm; a methylene at 1.5 & 1.63 ppm; $-\text{CH}_2$ at 2.38–2.43 ppm & 2.55 ppm and $-\text{CH}$ at 5.18–5.20 & 5.1 ppm (Wang et al., 2016; Masood et al., 2012; Wei et al., 2014). The ^1H NMR spectrum depict presence of HV unit in the PHAs. These signals clearly describe the presence of PHB-co-PHV in the extracted polymer.

3.4.3. Thermal characterization of PHAs

DTA analysis revealed that the T_m of extracted PHB-co-PHV was 166 °C (62 mj/mg ΔH ; endothermic reaction). However, the glass transition temperature (T_g) was not detected. The PHB-co-PHV degradation was observed between 100 and 400 °C and weight loss (%) was gradually increased with temperature. Remarkably, 0.4, 2.4, 61.2, and 93.0% weight loss of PHB-co-PHV was detected at 100, 248, 300 and 371 °C respectively (Fig. 6). Optimum thermal degradation (2.92 mg/min) was detected at 273 °C (T_d) as revealed from DTG curve (Fig. 6). Crystallinity (X_c) of extracted PHB-co-PHV was found to be 42.46%. Our results coincide with the thermal properties such as T_m (155 to 169 °C), T_d (284 °C) and X_c (46.2%) of PHB-co-PHV (Brunel et al., 2014). The T_m , X_c of extracted PHB-co-PHV is lower than the PHB-co-PHV reported earlier which indicated the polymer containing more amount of HB than HV. Hence this result depicting the amorphous part of this polymer will decompose faster however the crystalline part of this polymer can provide durability. The thermal and crystallinity characteristics confer the quality as well as the purity of the polymer.

3.4.4. X-ray diffraction analysis

The degree of crystallinity of PHB-co-PHV was estimated from X-ray diffractogram. The $2\theta^\circ$ values obtained at 12.96°, 16.37°, 24.91°, 26.62°, 28.83°, 35.35°, 38.86° and 42.68° (Fig. 7) are corresponding to PHB-co-PHV. Among all, five distinct peaks were observed at 12.96°, 16.37°, 35.35°, 38.86°, 42.68° and the high intense peak at 28.83° indicating crystalline nature of PHB-co-PHV. Our result also corroborates with the result of few other studies (Wei et al., 2014; Brunel et al., 2014) where the obtained absorbance points were similar.

3.4.5. Morphological analysis of PHAs film

PHB-co-PHV film exterior was uneven and fairly regular as confirmed by FE-SEM (Fig. 8b) and AFM (Fig. 8a) imaging, which indicating its bio-degradable nature. Rough exterior of PHB-co-PHV film supports tenderness of microbial cells and subsequently formation of pores (micro size) on the surface (Shah, 2012; Padernshoke et al., 2004). Further, crystalline nature (Spyros et al., 1997) of the PHAs film also boosts tenderness of microbes, fronting to degradation of polymer to CO_2 & H_2O in oxic and CO_2 & CH_4 in anoxic condition (Ym and Savitha, 2011).

3.4.6. Cytotoxicity assay

FACS assay data implied remarkable cell survivability between 91.02 and 65.58% and the death rate 6.74–31.31% in 100–500 $\mu\text{g}/\text{ml}$ of extracted PHB-co-PHV. However, cell survivability and death rate ranged from 81.86 to 73.40% and 11.27–18.50% in standard PHB (Fig. 9 & Table S4 in supplementary file). In general, higher cell survivability was perceived in extracted PHB-co-PHV than standing up to 400 $\mu\text{g}/\text{ml}$, which confirmed noncytotoxic nature of extracted PHB-co-PHV on adherent mouse fibroblast 3T3 cells. Moreover, cell viability above 50% is clear evident of noncytotoxic nature of PHAs (Mohapatra et al., 2016b). In corroboration to our result, noncytotoxic effect of P(3HB-co-3HDD-co-3HTD) and PHB recovered from *Lysinibacillus* sp. and *Bacillus subtilis* were also reported earlier (Mohapatra et al., 2016, 2017). Lower bioactivity and acidity than glycolic & lactic make PHB noncytotoxic to different cells (Chuah et al., 2013). Elevated cytocompatibility indicates

diverse applications of PHB-co-PHV, which could be exploited for various biomedical implications in future.

4. Conclusion

In this research, reorientation of PHAs (PHB-co-PHV) production from submerged to solid state fermentation was validated. Production of PHB-co-PHV through solid state fermentation increases purity, productivity and minimizes use of energy. Additionally, agar generated from the bioprocess technology can be reused for further applications, which balances overall economy of its production. This research established a novel noncytotoxic biopolymer PHB-co-PHV production (3.72 g/l) from *Bacillus megaterium* OUAT 016 through solid state fermentation. Further, presence of different proportions of HV monomers and rough surface of the extracted PHB-co-PHV supports microbial tenderness and greatly enhance the biodegradability performance. The low melting temperature and crystallinity of PHB-co-PHV depicted its toughness, impact resistance and flexibility over other polymers. As PHB-co-PHV is extremely less or null toxic to diversified cells, thereby indicating its aptness for several biomedical applications including as a drug delivery carrier. Hence, further research is highly indispensable prior to biomedical applications of the PHB-co-PHV.

Acknowledgement

This research did not receive grant from any funding agencies. The authors are thankful to Dr. S.K. Dash, Dr. S. Acharya, Dr. G.S. Acharya (OIC, CIF) and Dr. S. K. Pradhan, HoD, Department of Bioinformatics, OUAT, Bhubaneswar, Odisha for providing laboratory facilities during the period of research work. The authors have no conflict of interest to declare.

Appendix A. Supplementary material

Supplementary data to this article can be found online at <https://doi.org/10.1016/j.sjbs.2020.02.001>.

References

- Arikawa, H., Sato, S., Fujiki, T., Matsumoto, K., 2017. Simple and rapid method for isolation and quantitation of polyhydroxyalkanoate by SDS-sonication treatment. *J. Biosci. Bioeng.* 124, 250–254. <https://doi.org/10.1016/j.jbiosc.2017.03.003>.
- Bhagwati, P., Pradhan, S., Dash, H.R., Das, S., 2015. Production, optimization and characterization of polyhydroxybutyrate, a biodegradable plastic by *Bacillus* spp. *Biosci. Biotechnol. Biochem.* 79, 1454–1463. <https://doi.org/10.1080/09168451.2015.1034651>.
- Brunel, D.G., Pachekoski, W.M., Carla-Dalmolin, J.A.M.A., 2014. Natural additives for poly (hydroxybutyrate - CO - hydroxyvalerate) - PHBV: effect on mechanical properties and biodegradation. *Mater. Res.* 17, 1145–1156. <https://doi.org/10.1590/1516-1439.235613>.
- Chuah, J., Yamada, M., Taguchi, S., Sudesh, K., Doi, Y., Numata, K., 2013. Biosynthesis and characterization of polyhydroxyalkanoate containing 5-hydroxyvalerate units: effects of 5HV units on biodegradability, cytotoxicity, mechanical and thermal properties. *Polym. Degrad. Stab.* 98, 331–338.
- Desouky, S.E., El-Shiekh, H.H., Elabd, M.A., Shehab, A.M., 2014. Screening, optimization and extraction of polyhydroxyalkanoates (PHAs) from *Bacillus thuringiensis*. *J. Adv. Biol. Biotechnol.* 1 (1), 40–54.
- Gomaa, E.Z., 2014. Production of polyhydroxyalkanoates (PHAs) by *Bacillus subtilis* and *Escherichia coli* grown on cane molasses fortified with ethanol. *Braz. Arch. Biol. Technol.* 57 (1), 145–154.
- Holt, J.G., Krieg, N.R., Sneath, P.H.A., Stanley, J.T., Willium, S.T., 1994. *Bergey's Manual of Determinative Bacteriology*. Williams and Wilkins, Baltimore.
- Thatoi, H., Behera, B.C., Dangar, T.K., RanjanMishra, R., 2012. Microbial biodiversity in mangrove soils of bhitarkanika. Odisha. India. *Int. J. Environ. Biol.* 2, 50–58.
- Khiyami, M.A., Al-fadual, S.M., Bahklia, A.H., 2011. Polyhydroxyalkanoates production via *Bacillus* plastic composite support (PCS) biofilm and date palm syrup. *J. Med. Plants. Res.* 5 (14), 3312–3320.
- Kunasundari, B., Sudesh, K., 2011. Isolation and recovery of microbial polyhydroxyalkanoates. *Express Polym. Lett.* 5, 620–634. <https://doi.org/10.3144/expresspolymlett.2011.60>.

- Maity, S., Das, S., Samantaray, D.P., 2017. Effect of vitamin on accumulation of PHB by *Zobellella* species under submerged fermentation process. *Int. J. Curr. Microbiol. Appl. Sci.* 6, 1310–1316.
- Masood, F., Hasan, F., Ahmed, S., Hameed, P.C.A., 2012. Biosynthesis and characterization of poly-(3-hydroxybutyrate-co-3-hydroxyvalerate) from *Bacillus cereus* S10. *J. Polym. Environ.* 20, 865–871. <https://doi.org/10.1007/s10924-012-0457-y>.
- Mathews, D.H., Turner, D.H., 2002. Dynalign: An algorithm for finding the secondary structure common to two RNA sequences. *J. Mol. Biol.* 317, 191–203. <https://doi.org/10.1006/jmbi.2001.5351>.
- Mayeli, N., Motamedi, H., Heidarzadeh, F., 2015. Production of polyhydroxybutyrate by *Bacillus axaragansis* BIPC01 using petrochemical wastewater as carbon source. *Braz. Arch. Biol. Technol.* 58, 643–650. <https://doi.org/10.1590/S1516-8913201500048>.
- Mohapatra, S., Mohanta, P.R., Sarkar, B., Daware, A., Kumar, C., Samantaray, D.P., 2015. Production of polyhydroxyalkanoates (PHAs) by *Bacillus* strain isolated from waste water and its biochemical characterization. *Proc. Natl. Acad. Sci. USA*. <http://dx.doi.org/10.1007/s40011-015-0626-6>.
- Mohapatra, S., Rath, S.N., Pradhan, S.K., Samantaray, D.P., Rath, C.C., 2016a. Secondary structural models (16S rRNA) of polyhydroxyalkanoates producing *Bacillus* species isolated from different rhizospheric soil: phylogenetics and chemical analysis. *Int. J. Bioautomation* 20, 329–338.
- Mohapatra, S., Samantaray, D.P., Samantaray, S.M., 2014. Phylogenetic heterogeneity of the rhizospheric soil bacterial isolates producing PHAs revealed by comparative analysis of 16s-rRNA. *Int. J. Curr. Microbiol. App. Sci.* 3, 680–690.
- Mohapatra, S., Samantaray, D.P., Samantaray, S.M., Mishra, B.B., Das, S., Majumdar, S., Pradhan, S.K., Rath, S.N., Rath, C.C., Akthar, J., Achary, K.G., 2016b. Structural and thermal characterization of PHAs produced by *Lysinibacillus* sp. through submerged fermentation process. *Int. J. Biol. Macromol.* 93, 1161–1167. <https://doi.org/10.1016/j.ijbiomac.2016.09.077>.
- Mohapatra, S., Sarkar, B., Samantaray, D.P., Daware, A., Maity, S., Pattnaik, S., Bhattacharjee, S., 2017b. Bioconversion of fish solid waste into PHB using *Bacillus subtilis* based submerged fermentation process. *Environ. Technol.* 1–8. <https://doi.org/10.1080/09593330.2017.1291759>.
- Mravec, F., Obruca, S., Krzyzanek, V., Sedlacek, P., Hrubanova, K., Samek, O., Kucera, D., Benesova, P., Nebesarova, J., 2016. Accumulation of PHA granules in *Cupriavidus necator* as seen by confocal fluorescence microscopy. *FEMS Microbiol. Lett.* 363 (10), 1–18. <https://doi.org/10.1093/femsle/fnw094>.
- Israni, N., Shivakumar, S., 2013. Combinatorial screening of hydrolytic enzyme/s and PHA producing *Bacillus* spp. for cost effective production of PHAs. *Int. J. Pharma Bio. Sci.* 4, 934–945.
- Padermshoke, A., Sato, H., Katsumoto, Y., Ekgasit, S., Noda, I., Ozaki, Y., 2004. Thermally induced phase transition of poly(3-hydroxybutyrate-co-3-hydroxyhexanoate) investigated by two-dimensional infrared correlation spectroscopy. *Vib. Spectrosc.* 36, 241–249. <https://doi.org/10.1016/j.vibspec.2003.11.016>.
- Musa, H., Bolanle, B.B., Kasim, F.H., Arbain, D., 2016. Screening and production of polyhydroxybutyrate (PHB) by bacterial strains isolated from rhizosphere soil of groundnut plants. *Sains Malaysiana.* 45 (10), 1469–1476.
- Ramadas, N.V., Singh, S.K., Soccol, C.R., Pandey, A., 2009. Polyhydroxybutyrate production using agro-industrial residue as substrate by *Bacillus sphaericus* NCIM 5149. *Braz. arch. biol. technol.* 52 (1), 17–23. <https://doi.org/10.1590/S1516-89132009000100003>.
- Pandian, S.R.K., Deepak, V., Kalishwaralal, K., Rameshkumar, N., Jeyaraj, M., Gurunathan, S., 2010. Optimization and fed-batch production of PHB utilizing dairy waste and sea water as nutrient sources by *Bacillus megaterium* SRKP-3. *Bioresour. Technol.* 101, 705–711. <https://doi.org/10.1016/j.biortech.2009.08.040>.
- Rawte, T., Mavinkurve, S., 2002. A rapid hypochlorite method for extraction of polyhydroxyalkanoates from bacterial cells. *Ind. J. Exp. Biol.* 40, 924–929.
- Saitou, N., Nei, M., 1987. The neighbor-joining method- a new method for reconstructing phylogenetic trees. *Mol. Biol. Evol.* 4, 406–425.
- Sathiyarayanan, G., Kiran, G.S., Selvin, J., Saibaba, G., 2013. Optimization of polyhydroxybutyrate production by marine *Bacillus megaterium* MSBN04 under solid state culture. *Int. J. Biol. Macromol.* 60, 253–261. <https://doi.org/10.1016/j.ijbiomac.2013.05.031>.
- Sharma, P., Bajaj, B.K., 2016. Economical production of poly-3-hydroxybutyrate by *Bacillus cereus* under submerged and solid state fermentation. *J. Mater. Environ. Sci.* 7, 1219–1228.
- Shah, K.R., 2012. FTIR analysis of polyhydroxyalkanoates by novel *Bacillus* sp. AS 3–2 from soil of Kadi region, North Gujarat. *Ind. J. Biochem. Technol.* 3, 380–383.
- Shrivastav, A., Biotech, A., Kumar, S., Algallio, M., Private, B., 2014. Biodegradability studies of polyhydroxyalkanoate (PHA) film produced by a marine bacteria using *Jatropha* biodiesel. *World J. Microbiol. Biotechnol.* 27, 1531–1541. <https://doi.org/10.1007/s11274-010-0605-2>.
- Sindhu, R., 2015. Solid-state fermentation for the production of poly (hydroxyalkanoates). *Chem. Biochem. Eng. Q.* 29, 173–181 <https://doi.org/10.15255/CABEQ.2014.2256>.
- Singh, M., Kumar, P., Patel, S.K.S., Kalia, V.C., 2013. Production of polyhydroxyalkanoates co-polymer by *Bacillus thuringiensis*. *Int. J. Microbiol.* 53, 77–83.
- Singh, M., Patel, S.K.S., Kalia, V.C., 2009. *Bacillus subtilis* as potential producer for polyhydroxyalkanoates. *Microb. Cell Fact.* 8, 38–46.
- Spyros, A., Kimmich, R., Briese, B.H., Jendrossek, D., 1997. 1H NMR imaging study of enzymatic degradation in poly(3-hydroxybutyrate) and poly(3-hydroxybutyrate-co-3-hydroxyvalerate): evidence for preferential degradation of the amorphous phase by PHB depolymerase-B from *Pseudomonas lemoignei*. *Macromolecules.* 30, 8218–8225. <https://doi.org/10.1021/ma971193m>.
- Sultanpuram, M.T., Reddy, V., Mahmood, S.K., 2010. Production and characterization of PHB from two novel strains of *Bacillus* spp. isolated from soil and activated sludge. *J. Ind. Microbiol. Biotechnol.* 37, 271–278. <https://doi.org/10.1007/s10295-009-0670-4>.
- Tamura, K., Stecher, G., Peterson, D., Filipksi, A., Kumar, S., 2013. MEGA 6: molecular evolutionary genetics analysis version 6.0. *Mol. Biol. Evol.* 30, 2725–2729. <https://doi.org/10.1093/molbev/mst197>.
- Tan, G.Y., Chen, C.L., Li, L., Ge, L., Wang, L., Razaad, I., Li, Y., Zhao, L., Mo, Y., Wang, J.-Y., 2014. Start a research on biopolymer polyhydroxyalkanoate (PHA): A review. *Polymers (Basel).* 6, 706–754. <https://doi.org/10.3390/polym6030706>.
- Valappil, S.P., Peiris, D., Langley, G.J., Hermiman, J.M., Boccaccini, A.R., Bucke, C., Roy, I., 2007. Polyhydroxyalkanoate (PHA) biosynthesis from structurally unrelated carbon sources by a newly characterized *Bacillus* spp. *J. Biotechnol.* 127, 475–487. <https://doi.org/10.1016/j.jbiotec.2006.07.015>.
- Wang, C., Zheng, Y., Sun, Y., Fan, J., Qin, Q., Zhao, Z., 2016. Polymer chemistry mechanical properties and hemocompatibility. *R. Soc. Chem.* 7, 6120–6132. <https://doi.org/10.1039/c6py01131d>.
- Wei, L., Guho, N.M., Coats, E.R., McDonald, A.G., 2014. Characterization of poly(3-hydroxybutyrate-co-3-hydroxyvalerate) biosynthesized by mixed microbial consortia fed fermented dairy manure. *J. Appl. Polym. Sci.* 131 (11), 1–12. <https://doi.org/10.1002/app.40333>.
- Wu, H., Fan, Z., Jiang, X., Chen, J., Chen, G., 2016. Enhanced production of polyhydroxybutyrate by multiple dividing *E. coli*. *Microb. Cell Fact.* 15, 1–13. <https://doi.org/10.1186/s12934-016-0531-6>.
- Ym, V., Savitha, R., 2011. Microbial & biochemical technology overview on polyhydroxyalkanoates: A promising biopol. *J. Microbiol. Biochem. Technol.* 3 (5), 99–105. <https://doi.org/10.4172/1948-5948.1000059>.